Security Classification of This Report Has Been Cancelled

[redacted]

CHANDLER

Copy 214

[redacted]

RM A55L13a

NACA RM A55L13a

6478

TECH LIBRARY KAFB, NM
0143523

NACA

RESEARCH MEMORANDUM

Rig #1636C
FEB 195

HEAT-TRANSFER CHARACTERISTICS OF BLUNT TWO- AND THREE-DIMENSIONAL BODIES AT SUPERSONIC SPEEDS

By Glen Goodwin

Ames Aeronautical Laboratory
Moffett Field, Calif.

HADC
TECHNICAL LIBRARY
AFL 2811

[redacted]

NATIONAL ADVISORY COMMITTEE
FOR AERONAUTICS
WASHINGTON
February 16, 1956

[redacted]

[redacted]

Security Classification of This Report Has Been Cancelled

Classification cancelled (or changed to Unclassified)

By Authority of Nasa Tech Pub Announcement #45
(OFFICER AUTHORIZED TO CHANGE)

By ..... 11 May 61
NAME AND

.....
GRADE OF OFFICER MAKING CHANGE)

15 May 61
DATE

Security Classification of This Report Has Been Cancelled

TECH LIBRARY KAFB, NM
0143523

[redacted]

NATIONAL ADVISORY COMMITTEE FOR AERONAUTICS

RESEARCH MEMORANDUM

HEAT-TRANSFER CHARACTERISTICS OF BLUNT TWO- AND THREE-DIMENSIONAL BODIES AT SUPERSONIC SPEEDS

By Glen Goodwin

SUMMARY

Measured local- and average- heat-transfer coefficients on the front side of swept cylinders are presented for Mach numbers from 3.9 to 9.8, sweep angles from 0° to 70°, Reynolds numbers from 2,000 to 180,000, and ratios of wall temperature to stream stagnation temperature from 0.24 to 1.0. An analysis is presented which predicts the average heat-transfer coefficient on swept cylinders over this range of variables to an accuracy sufficient for most engineering purposes.

Local-heat-transfer coefficients are presented on hemispherically tipped cones and on a hemisphere-cylinder. The theory of Stine and Wanlass is shown to correlate well the data over a Mach number range from 3.9 to 6.9 and over a local Reynolds number range from 100 to 400,000 for these blunt bodies.

INTRODUCTION

High-speed flight of aircraft now contemplated has brought with it the problem of aerodynamic heating of the skin and structure of the aircraft. Two of the areas on the aircraft structure where the heating is most severe are on the leading edge of wings and on the nose of bodies.

In general, pointed shapes and sharp leading edges of the wings are advantageous in that they tend to reduce the drag of the configuration; however, pointed shapes and sharp leading edges of wings aggravate the heating problem because of two factors. The sharp pointed shapes accept heat from the hot boundary layer at a very high rate; it can be shown, for example, that the heat-transfer coefficient tends toward infinity at the point of a sharp object. Also, these sharp objects have little material with which to absorb and dissipate the incoming heat. One way out of this dilemma is to blunt the leading edge of wings and the nose of bodies. By this method, two advantages are achieved and one disadvantage is incurred.

[redacted]

[redacted]

Security Classification of This Report Has Been Cancelled

Blunting a leading edge reduces the local rate of heat transfer to it and provides material to absorb this incoming heat. Also, blunting provides space for a leading-edge cooling system. In addition, it provides some added strength at a point where thermal stresses tend to be high. Sweeping the blunt leading edge of a wing further reduces the local rate of heat transferred to it.

The main disadvantage of blunting is that it increases the pressure drag of the wing or body over that of a sharp-edged configuration. For wings, the leading-edge drag may be drastically reduced by sweeping the wing. It can be shown from experimental measurements and from theoretical considerations that the drag of the front side of a cylinder of unit length is reduced by a factor equal to the cube of the cosine of the sweep angle. For example, a cylinder of unit length swept 60° has only $12\frac{1}{2}$ percent of the drag of an unswept cylinder.

For bodies required to carry a given volume, it is shown in reference 1 that an optimum shape for minimum drag requires some blunting of the nose; and for certain applications, for example, a body which is required to enter the atmosphere at high speeds, a blunt shape may have great advantages over a pointed shape. This advantage is primarily due to the fact that a high-drag body slows down at high altitudes where the heat-transfer rate is relatively low and also to the fact that the heat-transfer coefficients on the nose of a blunt body are smaller than those on a sharp pointed body.

This paper considers the heat-transfer characteristics of both two- and three-dimensional bodies. The heat-transfer characteristics of two-dimensional bodies will be discussed first. The body chosen for analysis and for testing was a circular cylinder. This body was chosen because it represents a simple shape for a leading edge of a wing. Most of the experimental work available has been done at Reynolds numbers of 1.8×10^5 or lower and indicates the presence of a laminar boundary layer on the front side of cylinders. Therefore, the method used to calculate the heat-transfer coefficients will be to solve the laminar-boundary-layer equations.

Many solutions of these equations are available for the case where the cylinder is normal to the stream, and some work has been done for the case where the cylinder is swept with respect to the stream.

A summary of these theoretical investigations is shown in the following table:

[redacted]

Security Classification of This Report Has Been Cancelled

Investigator	Fluid properties	Sweep angle	Remarks
Squire	Constant	0°	$u_1 = cx$
Eckert and Drewitz	Constant	0°	$u_1 = cx^m$
Brown and Donoughe	Variable	0°	Small heat transfer
Cohen and Reshotko	Variable	0°	$U = cX^m$; $\frac{T_w}{T_\infty}$ variable
Crabtree	Variable	Small	$U = cX^m$
Beckwith	Variable	Variable	Integral method
Eggers, Hansen, and Cunningham	Variable	Variable	$x = 0$; $T_w \ll T_0$
Goodwin, Creager, and Winkler	Constant	Variable	Properties evaluated locally in application

Squire (see ref. 2) assumed constant fluid properties, neglected the pressure terms and the dissipation function, and obtained a solution to the laminar-boundary-layer equations over an unyawed cylinder where the velocity at the outer edge of the boundary layer is proportional to the distance from the stagnation point. This solution is, therefore, limited to low-speed flow and small temperature differences.

Eckert and Drewitz (ref. 3) assumed constant fluid properties and that the velocity at the edge of the boundary layer was proportional to some power of the distance from the stagnation point. (This is the so-called wedge-type flow solution.)

Brown and Donoughe (ref. 4) assumed essentially the same velocity distribution over the cylinder as that in reference 3, but allowed fluid properties to vary. Their solution is limited to zero sweep and small rates of heat transfer to the cylinder.

[redacted]

Security Classification of This Report Has Been Cancelled

Cohen and Reshotko (ref. 5) allowed fluid properties to vary and assumed that the velocity at the outer edge of the boundary layer could be expressed as $U = cX^m$. Their investigation was limited to zero sweep. They also investigated the effect of allowing the ratio of the wall temperature to the stream stagnation temperature to vary.

Crabtree (ref. 6) allowed fluid properties to vary and treated the case of a swept cylinder. His solution is valid only for small angles of sweep where the free-stream Mach number is high.

Beckwith (ref. 7) treated both variable fluid properties and variable sweep by using integral methods. These methods, however, lack generality. Eggers, Hansen, and Cunningham (ref. 8) allowed both properties and sweep angle to vary, but limited their analysis to the stagnation point on the cylinder and to the case where the cylinder temperature was negligible with respect to the stagnation temperature of the stream.

None of these investigations yielded an analytic expression for the heat transfer to the entire front side of a swept cylinder which would point out the effects of single variables or allow the correlation of all of the available experimental information. In an effort to find a solution which would do this, the subsequent analysis was performed.

SYMBOLS

a speed of sound, ft/sec

D cylinder diameter or diameter of hemispherical cone tip, ft

h local-heat-transfer coefficient, $\frac{\text{Btu}}{(\text{hr})(\text{sq ft})(^\circ\text{F})}$

k thermal conductivity of air, $\frac{\text{Btu}}{(\text{hr})(\text{sq ft})(^\circ\text{F/ft})}$

M Mach number

Nu_{av} average Nusselt number, $\frac{h_{av}D}{k_t}$

Nu_L local Nusselt number, $\frac{hD}{k_t}$

Security Classification of This Report Has Been Cancelled

Nu_x local Nusselt number, $\frac{hx}{k_1}$

p pressure, lb/sq ft

Pr Prandtl number

R_x local Reynolds number, $\frac{\rho_1 u_1 x}{\mu_1}$

R_2 Reynolds number evaluated behind normal shock wave, $\frac{\rho_\infty u_\infty D}{\mu_t}$

u fluid velocity, ft/sec

U transformed velocity at edge of boundary layer (see ref. 5)

x surface coordinate on cylinder or cone

X transformed surface coordinate on cylinder (see ref. 5)

Λ sweep angle, deg

ϕ azimuth angle on cylinder, deg

ρ density of air, slugs/cu ft

γ ratio of specific heats

μ viscosity of air, lb-sec/sq ft

Subscripts:

av average conditions

t reservoir or total conditions

1 conditions at outer edge of boundary layer at x

2 conditions just downstream of normal shock wave

∞ conditions in free stream

Security Classification of This Report Has Been Cancelled

ANALYSIS

The continuity, momentum, and total-energy equations for the laminar boundary layer over a swept cylinder were derived by using the order-of-magnitude arguments pointed out by Sears (ref. 9) for the continuity and momentum equations and by Crabtree (ref. 6) for the total-energy equation. This set of equations was solved under the following assumptions: The Prandtl number was unity, the velocity at the outer edge of the boundary layer was a linear function of the distance from the forward stagnation point, and the flow in the boundary layer was incompressible.

The solution to this set of equations was, then, identical with the solution obtained by Squire for the heat-transfer rate over a cylinder in subsonic flow.

This solution gave no hint as to where in the boundary layer the fluid properties should be evaluated. Some further assumptions were, therefore, made: The pressure was evaluated locally, and the viscosity and thermal conductivity of the air were linear functions of the temperature. It was also assumed that, for variable Prandtl number, the correction obtained by Cohen and Reshotko for the unswept cylinder would apply to the swept case.

The main results of the analysis which is given in detail in reference 10 are as follows:

The local Nusselt number for $Pr = 0.7$ is given by

$$Nu_L = \frac{hD}{k_t} = 0.73\sqrt{R_2 F(\Lambda,M)G(M)\Phi(\phi)} \tag{1}$$

where

$$F(\Lambda,M) = \frac{p_{x=0}}{p_{t_2}}\frac{a_{x=0}}{a_t}$$

$$G(M) = \frac{p_{t_2}}{p_\infty}\frac{a_\infty}{a_t}\frac{1}{M}$$

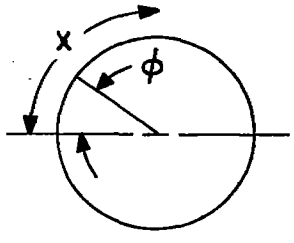

Security Classification of This Report Has Been Cancelled

$$\Phi(\phi) = \frac{p_x}{p_{x=0}} = \left[1 + \frac{\gamma - 1}{2}\left(2.13\,\frac{x}{D}\right)^2\right]^{\gamma/(\gamma-1)}$$

$$\frac{p_{x=0}}{p_{t_2}} = \cos^2\Lambda + \left[\frac{\left(\frac{2\gamma M^2}{\gamma + 1} - \frac{\gamma - 1}{\gamma + 1}\right)^{1/(\gamma-1)}}{\left(\frac{\gamma + 1}{2} M^2\right)^{\gamma/(\gamma-1)}}\right]\sin^2\Lambda$$

$$\frac{a_{x=0}}{a_t} = \left[1 - \frac{\frac{\gamma - 1}{2} M^2 \sin^2\Lambda}{1 + \frac{\gamma - 1}{2} M^2}\right]^{1/2}$$

The average Nusselt number over the front side of the swept cylinder is obtained by integrating equation (1) over the front side of the cylinder; therefore,

$$Nu_{av} = 0.52\sqrt{R_2 F(\Lambda,M) G(M)} \tag{2}$$

RESULTS AND DISCUSSION

Heat-Transfer Characteristics of Two-Dimensional Bodies

Before comparing these results with experimentally measured heat-transfer coefficients on swept cylinders, the pressure-ratio distribution over swept and unswept cylinders at high Mach numbers will be shown in order to assess the validity of the assumption that the velocity at the outer edge of the boundary layer varies linearly with the distance from the leading edge of the cylinder.

Figure 1 shows the ratio of the pressure on the surface of the cylinder to the pressure at the stagnation point plotted against azimuth angle for a cylinder normal to the stream. The experimental points are shown for a range of free-stream Mach numbers from 2.5 to 7 and over a

Security Classification of This Report Has Been Cancelled

range of Reynolds numbers from 6,700 to 140,000. The solid-line curve was calculated by assuming that the velocity at the outer edge of the boundary layer varied linearly with the distance along the surface from the stagnation point. It can be seen that the pressure-ratio distribution is unaffected by both free-stream Mach number changes from 2.5 to 7 and by Reynolds number variations from 6,700 to 140,000. Also, it can be seen from the agreement between the points and the solid-line curve that the assumption that the velocity varies linearly with surface distance is valid.

Figure 2 has the same quantities plotted as were shown in figure 1. In figure 2, however, the points were obtained at two Mach numbers, 3.9 and 6.9, but with angle of sweep varying from 0° to 60°. The solid-line curve is the same as that shown previously, and it can be seen that sweeping the cylinder did not change the pressure-ratio distribution over it. Thus, it can be concluded that at high Mach numbers the pressure-ratio distribution is a unique function of the azimuth angle only.

The actual pressure at the leading edge of a swept cylinder can be calculated with good accuracy by using Rayleigh's equation based upon the component of Mach number normal to the cylinder axis.

This fact and the fact that the pressure-ratio distribution can be calculated allow the effect of sweep on the pressure drag to be determined. The result for a unit-length cylinder is that the pressure-drag coefficient varies directly as the cube of the cosine of the sweep angle.

Since it has been shown (figs. 1 and 2) that the flow velocity at the outer edge of the boundary layer varies linearly with the surface distance for Mach numbers above 2.5, results of the analysis will now be compared with experimentally measured local-heat-transfer coefficients.

Figure 3 shows the ratio of the local-heat-transfer coefficient at any azimuth angle to that at the stagnation point as a function of azimuth angle. The points shown are measured values obtained at 0° sweep, 30° sweep, and 44° sweep. The experimental values were obtained in the Ames low-density wind tunnel at a Mach number of 3.9 and at Reynolds numbers from 2,100 to 6,700. The experimental method was to measure the heat transferred from a small plug which was thermally insulated from the test cylinder. The test plug was kept at the same temperature as the test body in order to avoid the complication of having to evaluate the effect of a variable surface temperature on the heat-transfer coefficient. A complete description of the test method is given in reference 10 and, for that reason, it will not be discussed further herein.

The experimental data exhibit some experimental scatter; but within the accuracy of the measurements, no definite trend of this ratio with sweep angle could be determined.

Security Classification of This Report Has Been Cancelled

The result of the analysis of reference 10 is shown by the solid-line curve, and it can be seen that this curve agrees reasonably well with the experimental points. Also, the analysis indicated no variation of this ratio with sweep angle.

For comparison, the theory of Cohen and Reshotko for a compressible boundary layer on an unswept cylinder is shown as the dashed-line curve. It can be seen that there is little difference between the two theories. The small difference is attributed to the fact that the local Mach number is relatively low over the cylinder; the local Mach number is always less than 2.0.

Sweeping the cylinder did not affect the ratio of the local-heat-transfer coefficient to that at the stagnation point of the cylinder, but it did affect the level of the data and this effect is shown in figure 4. In this figure the ratio of the average Nusselt number over the front half of the cylinder divided by the average Nusselt number at zero sweep is plotted against the sweep angle. The circular symbols shown at 30° sweep and 44° sweep were obtained in the Ames low-density wind tunnel at a Mach number of 3.9, and the square symbols were obtained at the Langley 11-inch hypersonic tunnel at a Mach number of 6.9. (The latter tests were reported in ref. 11.) It can be seen that sweeping the cylinder reduced the heat transfer to it; at 60° sweep the Nusselt number is reduced to one-half of its no-sweep value. The solid-line curve is the result of the analysis evaluated at a Mach number of 3.9, and the dashed-line curve is the result of the analysis evaluated at a Mach number of 6.9. It can be seen that, up to sweep angles of about 45°, the analysis predicts the experimental data well. However, for sweep angles above 45°, the analysis predicts more of a decrease of the Nusselt number with sweep than is actually measured experimentally. The departure of the data from the theory at sweep angles above 45° is also corroborated by the tests reported in reference 8.

The temperature-recovery factors were also reduced by sweep; however, the reduction is small compared with the reduction in Nusselt number. Measured recovery factors on the front half of swept cylinders were 0.924, 0.924, 0.900, and 0.888 for sweep angles of 0°, 20°, 40°, and 60°, respectively. These values were measured at a Mach number of 6.9.

One of the results of this analysis is that it yields a correlation parameter whereby the average Nusselt number over the front half of the cylinder can be correlated over a wide range of free-stream Mach numbers, Reynolds numbers, and sweep angles. Figure 5 shows this correlation. In this figure the average Nusselt number evaluated at stagnation temperature for the front half of swept cylinders is plotted against the correlation parameter given by the analysis. This correlation parameter is defined in equation (1). The circular symbols shown at the upper

Security Classification of This Report Has Been Cancelled

right-hand corner of figure 5 were obtained in the Langley 11-inch hypersonic tunnel at a Mach number of 6.9, a ratio of wall temperature to stagnation temperature from 0.5 to 1.0, and a range of sweep angles from 0° to 60°. The square symbols shown in about the center of the chart were obtained in the Ames low-density wind tunnel at a Mach number of 3.9 and a wall temperature equal to stagnation temperature for three sweep angles - 0°, 30°, and 44°. The diamond symbols shown toward the lower left-hand side of figure 5 were obtained in the Ames gun tunnel at a Mach number of 9.8, a ratio of wall temperature to stagnation temperature of 0.24, and a range of sweep angles from 0° to 70°. The data shown in this figure represent a Reynolds number range from 315 for some of the points taken in the gun tunnel to 180,000, which corresponds to the Reynolds number obtained in the Langley 11-inch hypersonic tunnel. The solid-line curve shown in figure 5 is the result, given by equation (2). It can be seen that the analysis represents the data well.

The data shown in figure 5 were obtained over a range of stream stagnation temperatures from room temperature to 2,200° R and over a range of ratios of body temperature to stream stagnation temperature from 0.24 to 1.0. These data, then, represent flight temperature conditions up to flight Mach numbers of about 5.0. Although boundary-layer theory for unswept cylinders indicated that the analysis shown is conservative at higher flight Mach numbers, this indication has not been checked by experiment.

The data shown in figure 5 represent the case where the boundary layer on the cylinder was laminar. Some very recent (unpublished) measurements by Beckwith indicate that, if the free-stream Reynolds number is sufficiently high, sweeping the cylinder will cause transition to turbulent flow in the boundary layer and will cause the heat-transfer coefficients to be increased by sweep. The flight Reynolds number at which transition can be triggered by sweep is as yet undetermined.

Heat-Transfer Characteristics of Three-Dimensional Bodies

Local-heat-transfer coefficients have been measured on hemispherically tipped cones and on a hemisphere-cylinder. Figure 6 shows these data. In this figure the ratio of the local-heat-transfer coefficient to that at the stagnation point is plotted along the ordinate. The distance along the surface of the cone from the stagnation point, divided by the diameter of the hemispherical tip, is shown along the abscissa.

The cones were tested in the Ames low-density wind tunnel at a Mach number of 3.9, and the hemisphere-cylinder was tested in the Langley 11-inch hypersonic tunnel at a Mach number of 6.9. It can be seen that the heat-transfer-coefficient ratios are highest on the noses of these bodies but fall rapidly as the distance from the nose increases.

Security Classification of This Report Has Been Cancelled

The heat-transfer-coefficient ratio measured on the nose of the hemisphere-cylinder agrees well with that measured on the hemispherical nose of the $22\frac{1}{2}^{\circ}$ half-angle cone. This trend was not followed on the bluntest cone. On the bluntest cone, the heat-transfer-coefficient ratio on the nose was lower than that for the other bodies except very near the stagnation point. The nose-cone juncture of the bodies is shown by the vertical lines in figure 6, for example, at $x/D = 0.785$ for the hemisphere-cylinder.

The same general method will be used to calculate the heat-transfer coefficients over the blunt bodies as was used to calculate the heat-transfer coefficients over unswept cylinders. The main difference is that now the flow in the boundary layer is three-dimensional. However, three-dimensional axisymmetric boundary-layer equations can be transformed by use of Mangler's transformation to an equivalent set of two-dimensional equations. This has been done by Stine and Wanlass (ref. 12) and by Cohen and Reshotko (ref. 5). The main simplifying assumption used in these analyses is that the velocity at the outer edge of the boundary layer can be expressed as some power of the distance from the forward stagnation point. However, in an actual case, the velocity at the outer edge of a boundary layer does not vary in this fashion except very near the forward stagnation point. In the application of these analyses to real problems, the exponent is evaluated locally from measured pressure-distribution data.

Data obtained on these blunt bodies of revolution are shown in figure 7 in nondimensional form. In this figure, the local Nusselt number is plotted along the ordinate. The product of the local Reynolds number and a function of body shape and pressure distribution is plotted along the abscissa. The solid-line curve is the result given by the Stine and Wanlass analysis (ref. 12). The circular symbols were obtained on the bluntest cone and the square symbols were obtained on the less blunt cone. The diamond symbols were obtained on the hemisphere-cylinder.

It can be seen that the data are well correlated by this method over a range of local Reynolds numbers from 100 to 400,000 and at Mach numbers of 3.9 and 6.9. Also, a wide range of blunt body shapes is covered.

The correlation parameter plotted along the abscissa of figure 7 is taken from the analysis of Stine and Wanlass and is equal to

$$f\left(\frac{x}{D}, \frac{p_x}{p_{x=0}}\right) = \frac{Nu_x}{\sqrt{R_x}} \tag{3}$$

which is given by equations (2) to (7) in reference 12.

Security Classification of This Report Has Been Cancelled

Heat-transfer coefficients were also determined for the 55° half-angle hemispherically tipped cone at angle of attack. The results of these tests are shown in figure 8. In this figure are plotted along the ordinate the ratio of the local-heat-transfer coefficients divided by the value at the stagnation point on the body for the case when the body was at zero angle of attack. The distance along the surface of the cone divided by the tip diameter, denoted by x/D, is plotted along the abscissa of figure 8. Positive values of x/D shown on the right-hand side of this figure represent the windward side of the body, and negative values of x/D shown at the left-hand side of the figure represent the other side of the body. It can be seen that the heat-transfer coefficients over the hemispherical nose were not markedly altered by angles of attack of 12° and 24°. However, the heat-transfer coefficients on the conical section were increased by angle of attack on the windward side of the body and were considerably decreased on the other side of the body. It was found, however, that, on an average basis, angle-of-attack variations up to 24° did not appreciably change the total amount of heat transfer to the body.

CONCLUDING REMARKS

It can be concluded from the data presented herein that the theoretical methods appear adequate to predict the heat-transfer coefficients on the noses of blunt bodies and on the front side of swept cylinders over a wide range of Mach numbers and Reynolds numbers up to flight temperature conditions corresponding to flight at Mach numbers of approximately 5, provided the boundary-layer flow is laminar.

Ames Aeronautical Laboratory
National Advisory Committee for Aeronautics
Moffett Field, Calif., Nov. 3, 1955

Security Classification of This Report Has Been Cancelled

REFERENCES

1. Eggers, A. J., Jr., Dennis, David H., and Resnikoff, Meyer M.: Bodies of Revolution for Minimum Drag at High Supersonic Airspeeds. NACA RM A51K27, 1952.

2. Squire, H. B.: High Speed Flow. Heat Transfer. Vol. II of Modern Developments in Fluid Dynamics, ch. XIV, L. Howarth, ed., The Clarendon Press (Oxford), 1953, pp. 757-853.

3. Eckert, E., and Drewitz, O.: Calculation of the Temperature Field in the Laminar Boundary Layer of an Unheated Body in a High Speed Flow. R.T.P. Translation No. 1594, British Ministry of Aircraft Production. (From Luftfahrtforschung, vol. 19, no. 6, June 20, 1942, pp. 189-196.)

4. Brown, W. Bryon, and Donoughe, Patrick L.: Tables of Exact Laminar-Boundary-Layer Solutions When the Wall Is Porous and Fluid Properties Are Variable. NACA TN 2479, 1951.

5. Cohen, Clarence B., and Reshotko, Eli: Similar Solutions for the Compressible Laminar Boundary Layer With Heat Transfer and Pressure Gradient. NACA TN 3325, 1955.

6. Crabtree, L. F.: The Compressible Laminar Boundary Layer on a Yawed Infinite Wing. Aero. Quarterly, vol. V, July 1954, pp. 85-100.

7. Beckwith, Ivan E.: Theoretical Investigation of Laminar Heat Transfer on Yawed Infinite Cylinders in Supersonic Flow and a Comparison With Experimental Data. NACA RM L55F09, 1955.

8. Eggers, A. J., Jr., Hansen, C. Frederick, and Cunningham, Bernard E.: Theoretical and Experimental Investigation of the Effect of Yaw on Heat Transfer to Circular Cylinders in Hypersonic Flow. NACA RM A55E02, 1955.

9. Sears, W. R.: The Boundary Layer of Yawed Cylinders. Jour. Aero. Sci., vol. 15, no. 1, Jan. 1948, pp. 49-52.

10. Goodwin, Glen, Creager, Marcus O., and Winkler, Ernest L.: Investigation of Local Heat-Transfer and Pressure-Drag Characteristics of a Yawed Circular Cylinder at Supersonic Speeds. NACA RM A55H31, 1956.

11. Feller, William V.: Investigation of Equilibrium Temperature and Average Laminar Heat-Transfer Coefficients for the Front Half of Swept Circular Cylinders at Mach Number of 6.9. NACA RM L55F08a, 1955.

Security Classification of This Report Has Been Cancelled

12. Stine, Howard A., and Wanlass, Kent: Theoretical and Experimental Investigation of Aerodynamic-Heating and Isothermal Heat-Transfer Parameters on a Hemispherical Nose With Laminar Boundary Layer at Supersonic Mach Numbers. NACA TN 3344, 1954.

Security Classification of This Report Has Been Cancelled

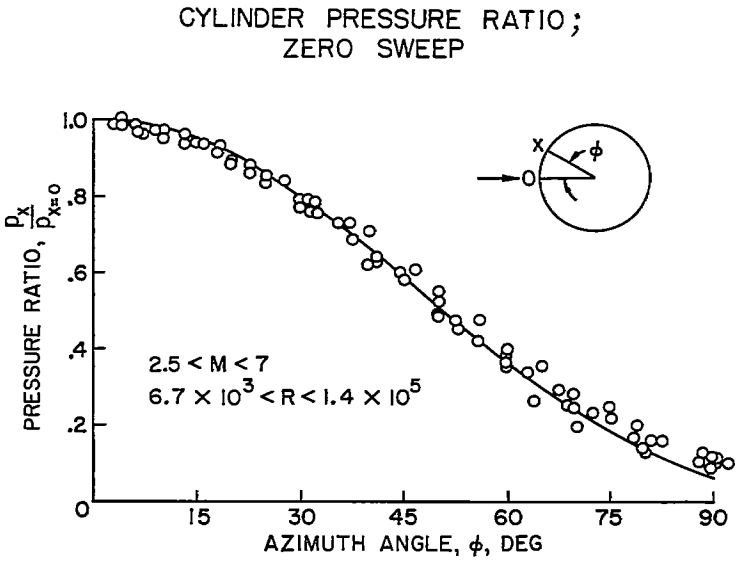

Figure 1

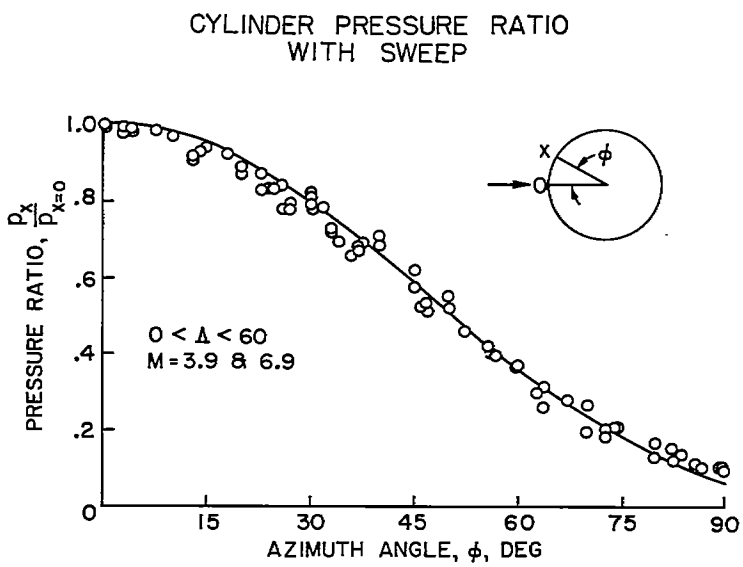

Figure 2

Security Classification of This Report Has Been Cancelled

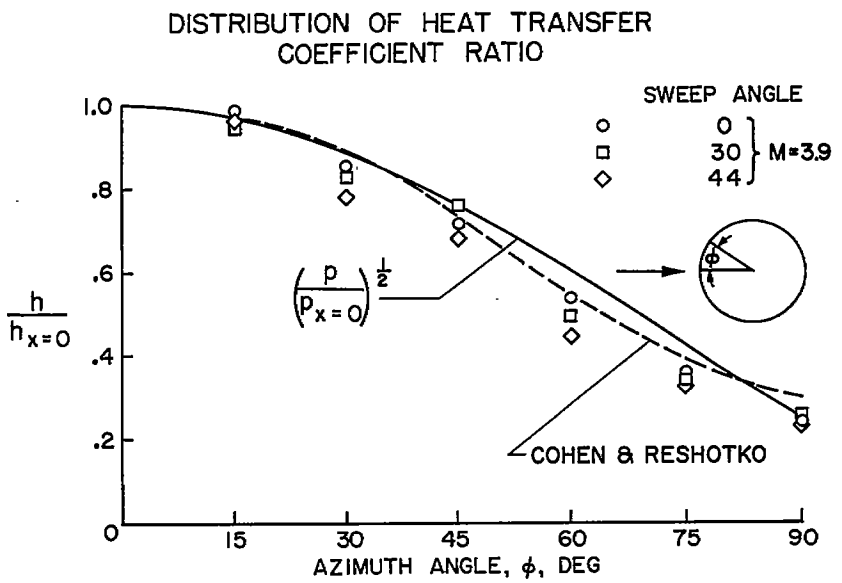

Figure 3

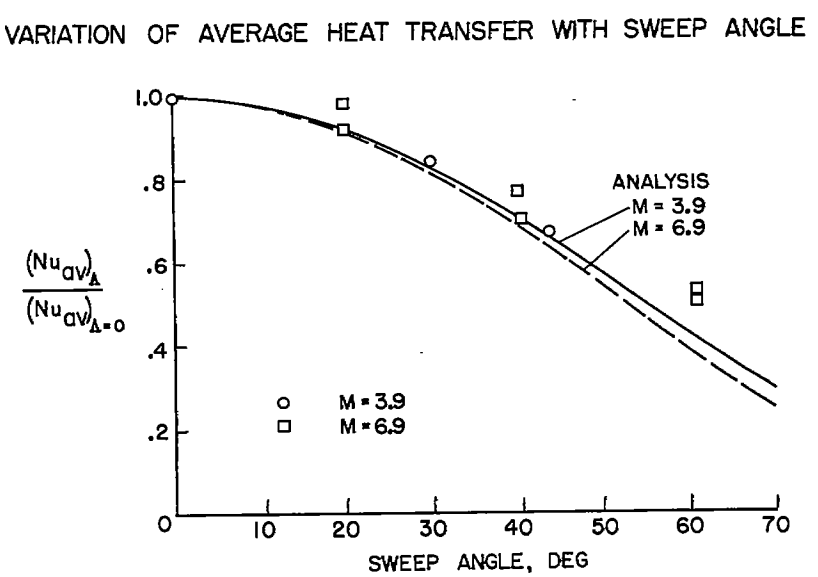

Figure 4

Security Classification of This Report Has Been Cancelled

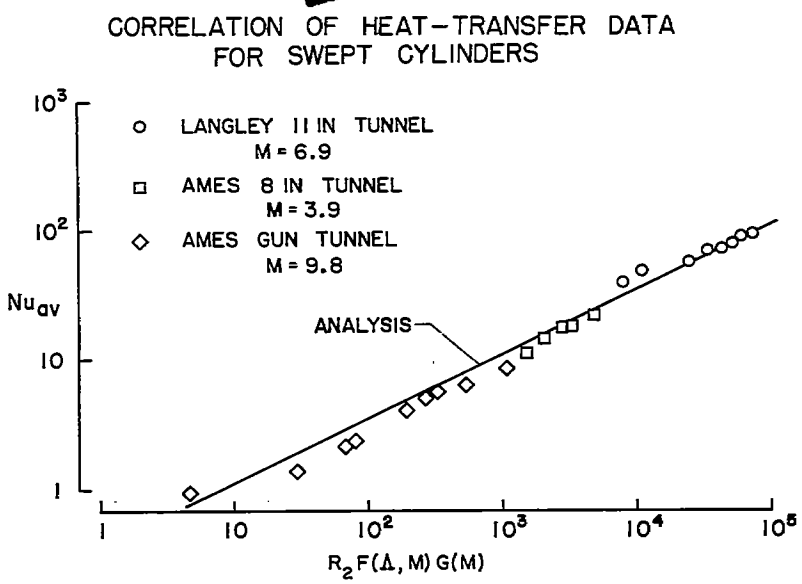

Figure 5

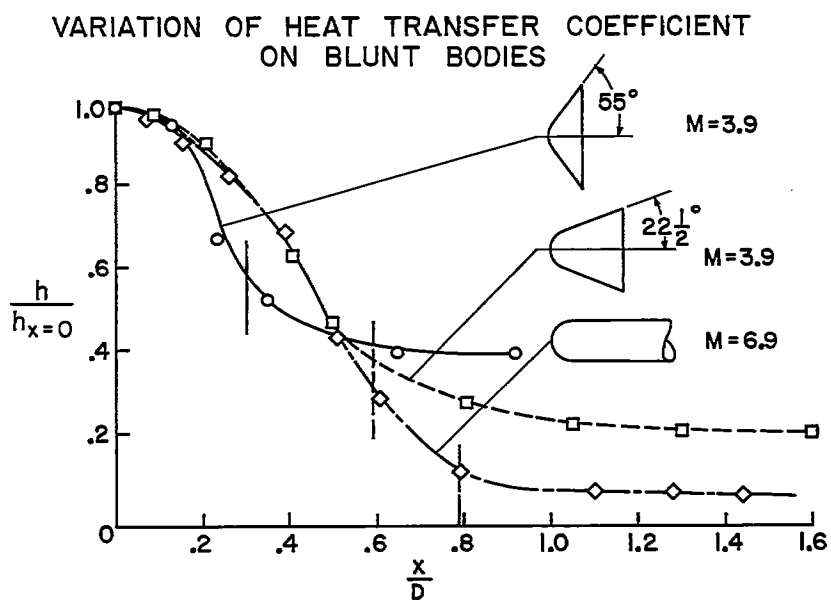

Figure 6

Security Classification of This Report Has Been Cancelled

LOCAL HEAT TRANSFER ON BLUNT BODIES

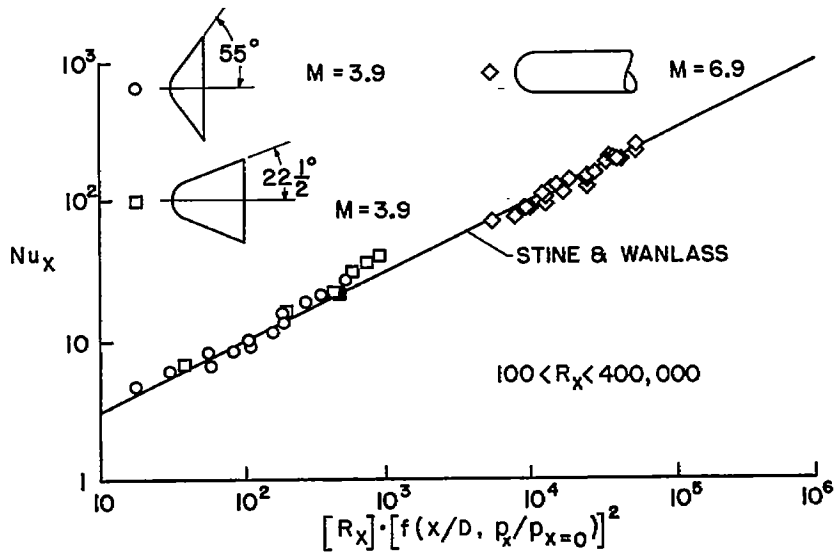

Figure 7

VARIATION OF HEAT TRANSFER COEFFICIENT ON BLUNT CONE

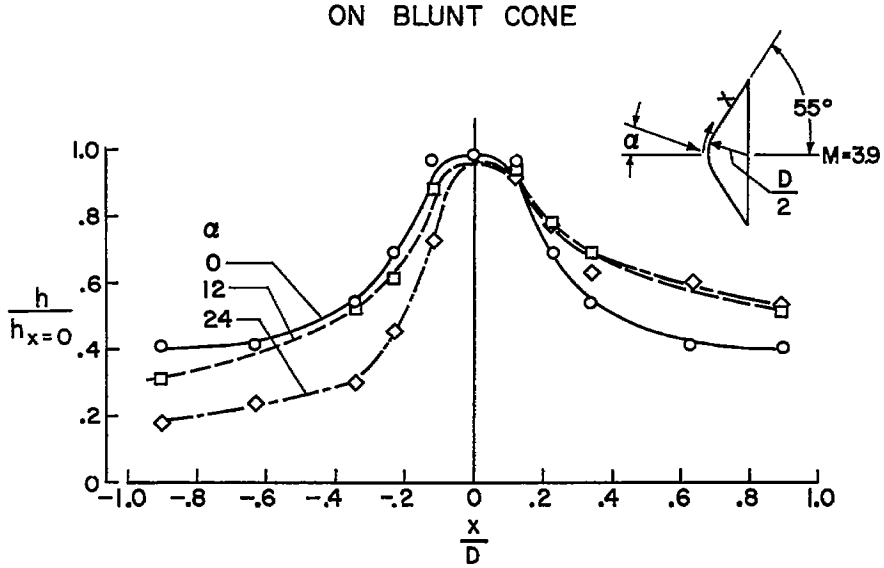

Figure 8